ANALYSES OF DISTRIBUTED ABSORBED POWER RESPONSES OF THE HUMAN HAND-ARM SYSTEM IN THE BENT- AND EXTENDED-ARM POSTURES

Surajudeen Adewusi[1], Subhash Rakheja[1], and Pierre Marcotte[2]
[1]CONCAVE Research Center, Concordia University, Montréal, Québec, Canada H3G 1M8
[2] Institut de recherche Robert-Sauvé en santé et en sécurité du travail (IRSST), 505 de Maisonneuve West, Montréal, Québec, Canada H3A 3C2

1. INTRODUCTION

The absorbed power P within the hand-arm system relates to mechanical stimulus attributed to vibration exposure, and has been suggested as an important biodynamic measure for assessing the vibration exposure (Lindstrom, 1975). The majority of studies, however, have been limited to total power derived from the responses at the driving-point. In a recent study, the distributed power was estimated using lumped-mass models with a fixed shoulder condition (Dong et al., 2007), although relatively high magnitudes of vibration of the shoulder and the head have been reported, particularly in the extended-arm posture (Sakakibara et al., 1986).

The absorbed power derived from lumped-mass models based upon driving-point measure may not adequately characterize deformations and energy absorption associated with vibration modes of individual hand-arm substructures, and cannot reveal posture effects. In this study, biomechanical models of the hand-arm system in the bent- and extended-arm postures subject to z_h-axis vibration are applied to derive the energy distribution within different substructures of the hand-arm system. The validity of the model was established on the basis of multiple simultaneously measured biodynamic responses, namely the driving-point impedance, vibration transmitted to different hand-arm segments and the total power absorbed.

2. METHODS

The formulation and structures of the hand-arm models in the bent- and extended arm postures are similar to those reported by Adewusi et al. (2010). The models incorporate a clamp-like structure of the hand with two-driving points formed by the finger and palm sides of the hand (Dong et al., 2007), together with representations of the upper- and fore-arms, wrist, elbow and shoulder joints, and the torso. The torso facilitated the study of shoulder motion and coupling between the hand-arm and the whole-body vibrations. The parameters of the models were derived on the basis of both the driving-point impedance and vibration transmitted to different segments of the hand-arm measured, using six subjects under broadband random excitation. The vibration of a chipping hammer operated in an energy dissipater was also measured in the laboratory. The distributed power of the models is evaluated under broadband random and chipping hammer excitations for the two postures.

The distributed power absorbed in a substructure at joint k (k = 1, … n), P_k, is estimated from the power dissipated in the damping elements of the substructure, such that:

$$P_k(f) = c_k\left[\Delta v_k(f)\right]^2 + C_k\left[\Delta\Omega_k(f)\right]^2 \tag{1}$$

where f is the frequency of vibration in Hz, Δv_k and $\Delta\Omega_k$ are relative translational and rotational rms velocities across the damping element at joint k, respectively, and c_k and C_k are the linear and rotational damping coefficients of joint k, respectively.

The total power, P, corresponding to frequency f is derived upon summation of the distributed power:

$$P(f) = \sum_{k=1}^{n} P_k(f) \tag{2a}$$

$$P_m(f) = Re\left[MI(f)\right]\cdot\left|v(f)\right|^2 \tag{2b}$$

where n is the number of damping elements in the model. The computed P was compared with the total power P_m estimated from the measured mechanical impedance MI and velocity v to further demonstrate the validity of the models.

Finally, the overall power of the models ($\overline{P}$) and that derived from the measured data over the entire frequency range of interest (with f_l and f_u as the lower and upper bounds) are derived from:

$$\overline{P} = \sum_{f_l}^{f_u} P(f_i) \tag{3}$$

3. RESULTS AND DISCUSSION

Figure 1 shows the distributed and total power responses of the hand-arm system models under random excitations for both the postures, while Figure 2 presents the power due to chipping hammer excitation for the bent-arm posture only. Figure 1 shows that the total power of the models is comparable with that derived from the measured data, which further confirmed the validity of the models. The validation of models on the basis of MI and transmissibility responses had been previously presented (Adewusi et al., 2010).

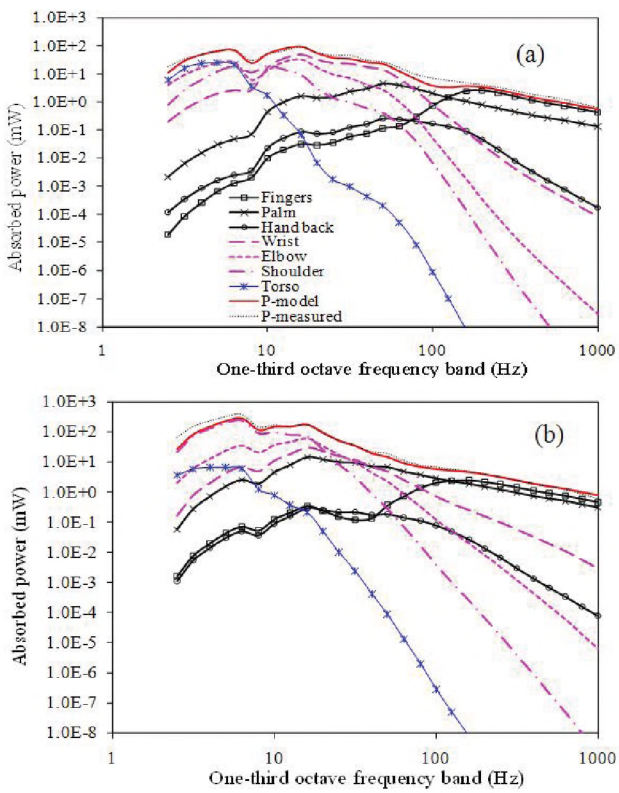

Figure 1. Distributed and total power absorbed in the human hand-arm due to broadband random excitation: (a) bent-arm posture; (b) extended-arm posture.

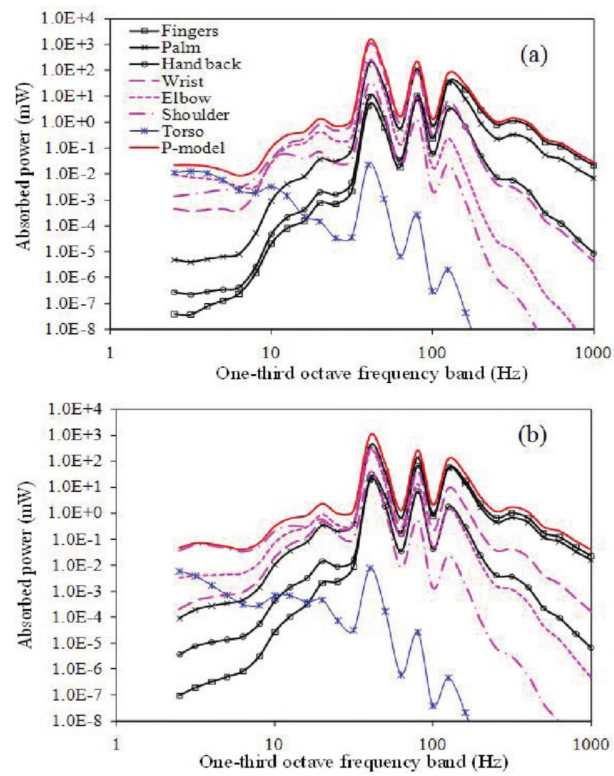

Figure 2. Distributed and total power absorbed in the human hand-arm due to chipping hammer excitation: (a) bent-arm posture; (b) extended-arm posture.

The figures show significant effect of excitation and posture on the absorbed power. Although Figure 2 shows that power is concentrated around the operating frequency (43.7 Hz) of the power tool, the trends shown by the power absorbed in different segments are similar for both excitations and postures. The results showed a general trend that the power absorbed in the arms (wrist, elbow and shoulder) was greater below 25 Hz than that in the hand (fingers, palm and hand back). The absorbed power of the hand structures was, however, greater above 100 Hz, except in the extended-arm posture, where the wrist power was greater than that of the hand back.

Despite similarities in trends shown by segmental absorbed power, the values of absorbed power in the extended arm posture were significantly greater than those in the bent-arm posture for the same overall frequency-weighted vibration. Under broadband random vibration with frequency weighted acceleration value of 5.25 m/s^2 (32.0 m/s^2 un weighted) in the 2.5 – 1000 Hz frequency range, the overall total power ($\overline{P}$) for the bent- and extended-arm postures were computed as 0.67 and 1.63 W, respectively. Furthermore, the frequencies of peak power under random excitation (Fig. 1) were close to resonance frequencies of the hand-arm system, while those due to chipping hammer excitation were dominated by the tool's operating frequency, its harmonics and resonant frequencies. The results showed that the power in different segments differed considerably, not only with posture but also in magnitudes and dominant frequencies, suggesting that different frequency-weightings may be needed to assess injury risks of different segments of the hand-arm system.

REFERENCES

Adewusi, S. A., Rakheja, S., and Marcotte, P. (2010). "Bio-dynamic Model of the Hand-arm System to Simulate Distributed Biodynamic Responses," *3rd American Conf. on Human Vibration*, Iowa City, Iowa, USA, June 1-4, 56-57.

Dong, J. H., Dong, R. G., Rakheja, S., Welcome D. E., McDowell T. W., and Wu J. Z. (2007). "A method for analyzing absorbed power distribution in the hand and arm substructures when operating vibration tools," J. Sound Vib., **311**, 1286–1304.

Lindstrom, I. M., (1975). "Vibration injury in rock drillers, chiselers, and grinders. Some views on the relationship between the quantity of energy absorbed and the risk of occurrence of vibration injury," *Proc. of.the 2nd Int. Hand-Arm Vibration Conf.*, Cincinnati, OH, pp. 77–83.

Sakakibara, H., Kondo, T., Miyao, M., Yamada, S., Nakagawa, T., Kobayashi, F., and Ono, Y. (1986). "Transmission of hand-arm vibration to the head," Scand. J. Work Environ. Health, **12**, 359–361.